

Process and resolution impacts on UK coastal wave predictions from operational global-regional wave models

Andrew Saulter, Chris Bunney, Jian-Guo Li and Tamzin Palmer

Met Office; FitzRoy Road, Exeter, Devon, UK, EX1 3PB

Contact email: andrew.saulter@metoffice.gov.uk

Abstract

UK coastal waters comprise a complex mix of embayments, areas with shallow bathymetry and strong tides. Recent developments in supercomputing capacity and wave model grid schemes make it possible to consider issuing wave forecasts for these waters, direct from configurations that have been more generically developed for global and regional forecast applications but also aim to adequately resolve the coastal zone.

This study assesses how close the present generation of wave models run operationally at the Met Office are to achieving this aim, using a comparison against in-situ observations covering both offshore and coastal waters around the UK. The configurations tested are: a global wave model using a Spherical Multiple Cell (SMC) grid with refinement up to 3km resolution around the UK; a 7km regular grid model mainly designed for offshore forecasting for the northwest European continental shelf seas, but which incorporates the effects of mesoscale surface currents; and a 3-1.5km SMC grid model for UK waters including forcing by surface currents at a similar resolution.

Increasing resolution and application of currents in the models yields little positive impact in the offshore zone; implying that the dominant source of error results from a combination of uncertainty in wind forcing and model source terms. In the coastal zone, the high resolution model including currents obtains the best overall results for significant wave height. For parameters with a higher sensitivity to the distribution of energy through the wave spectrum, such as peak and zero-upcrossing period, the skill of all models is generally poor in the coastal zone when using the simple metrics in this study. In relative terms, the skill achieved in the coastal zone lags performance offshore, implying the need to further develop the coastal component of such models and to discriminate between offshore and coastal observations when validating such configurations.

1. Introduction

Historically, large area wave models run operationally by National Meteorological Services have been limited in scope to generating information at meso-scales (5-10km) for regional applications and scales of several 10s of kilometres for global systems. As a result, the forecasts provided by these models are only generically appropriate for open waters well away from the coast and, therefore, are principally aimed at professional mariners. From a public safety perspective such data

are of limited use, since the majority of leisure mariners are likely to restrict their activities to within a few kilometres of the coast. Besides, there is a recognised need for wave information directly at the coast in support of coastal flood forecast and beach safety applications.

Increasing computing resources and improvements in model numerical schemes and shallow water parameterizations suggest that over the next decade, a transition toward operational running of large area wave modelling systems that resolve the coastal zone at a useful level of detail is feasible. There are a number of choices as to how such systems could be set up. For example, model nesting enables a 'distributed' set of coastal zone models to be coupled with a coarser large area model (Tolman, 2008); such systems have the advantage of being able to spread the modelling load across a network of processors or computers, but carry the overhead of maintaining a large number of model configurations. An alternative solution is to adopt a form of model in which cell sizes are not uniform and resolution is maximised close to the coast whilst being coarser in less complex offshore regions (e.g. curvilinear, Doorn and Ris, 1998; unstructured triangular mesh, Roland et al., 2009; or spherical multiple-cell grids, Li 2012). For these models the advantage is in working with a single, seamless, configuration. However, adopting such an approach puts an emphasis on model optimisation and tuning parameterizations such that forecast performance is of high quality across the whole model domain.

In terms of processes, models that resolve the coastal zone must pay specific attention to not only shallow water effects on the waves, but also to the detail of wave propagation where the orientation of the coastline changes (Cavaleri and Sclavo, 1998) and the variability in the wave field introduced through wave interaction with tidal currents. Strong currents and current shears in coastal waters have been noted to have significant effects on wave conditions both local to the current and downstream. For example, Palmer and Saulter (2016) found significant tidal cycle variability in wave conditions at Rustington, in the English Channel, due to refraction of swell across (sheared) tidal currents further offshore. Ardhuin et al. (2017) note a significant effect due to detailed current structures offshore, which potentially affects the waves propagating into the nearshore zone.

In this study the performance of three models, which represent state of the art operational wave forecast systems run at the Met Office, is reviewed against coastal zone observations from around the UK and contrasted against performance further offshore. The environment and distribution of observations in UK waters provides an excellent test of coastal performance due to a complex mix of embayments, areas with shallow bathymetry and strong tides. The modelling systems, which vary in terms of grid definition and use of surface current boundary conditions, are described in section 2. Section 3 describes the trial period, observation datasets and performance evaluation method. Results of the intercomparison of model performance for both offshore and coastal zones is presented in Section 4, and the benefits of variations in model set up and overall ability of the models to provide a useful coastal zone forecast are discussed in Section 5.

2. Models

2.1 Codebases

The wave models run for this study were all based on the WAVEWATCH III community model code at version 4.18 (Tolman et al., 2009). Surface current data were generated using runs of the NEMO ocean circulation model (Madec, 2008) at version 3.6.

2.2 Configurations

The wave configurations are summarised in Table 1. In all cases the models were driven by winds from the Met Office operational atmosphere model's analysis, with a horizontal resolution of approximately 17km. The nested models described in sections 2.2.2 and 2.2.3 use spectral boundary conditions provided from the global wave model described in section 2.2.1. In all cases the wave source terms were based on the ST4 switch in WAVEWATCH III following Ardhuin et al. (2010) and nonlinear terms used the Discrete Interaction Approximation (DIA) package following Hasselmann et al. (1985). Shallow water physics were applied, with JONSWAP gamma for bottom friction (Hasselmann et al., 1973) set to 0.038 and depth induced wave breaking coefficient based on the Battjes and Janssen (1978) scheme limited to 0.2.

Table 1. Summary of wave model configurations

Configuration Name	Domain Coverage	Grid Type (lat-lon)	Resolution(s)	Surface Current (resolution)	ST4 BETAMAX
S36125	Global	SMC	25-12-6-3km	No	1.36
AMM7CO6	NW European Shelf	Regular	7km	7km	1.45
UKSCO7	NW European Shelf	Rotated pole SMC	3-1.5km	3km	1.45

2.2.1 Global 25-12-6-3km model

The global wave model configuration (S36125) uses a Spherical Multiple-Cell grid (SMC; Li, 2011, 2012), with four levels of refinement. Cell resolution is approximately 25km at mid-latitudes in the open ocean, with refinement to 12km and 6km at coastlines worldwide. As a region of special interest, the northeast Atlantic and European seas are covered at an increased resolution of 12km in open waters, whilst the UK coastline is resolved using an additional level of refinement based on 3km cells. The propagation scheme associated with the SMC model grid is based on a 2nd order upstream non-oscillatory scheme (UNO2, Li, 2008) with Garden Sprinkler Effect (GSE) alleviation based on a hybrid swell age diffusion and averaging scheme (WAVEWATCH III Development Group, 2016). The ST4 tuning parameter BETAMAX was set to 1.36 in order to optimise performance globally, but otherwise version 4.18 default values were used. In this global configuration no surface currents are applied.

2.2.2 Atlantic Margin 7km model

The 7km Atlantic Margin Model (AMM7CO6) has been built to provide forecasts out to a lead time of 6 days ahead for the Copernicus Marine Environment Monitoring Service (<http://marine.copernicus.eu/>) and, as such, uses a grid that is matched with the NEMO shelf seas model used to provide ocean data for that service. This is a regular latitude-longitude set up, covering the region 40°N, 20°W to 65°N, 13°E. Propagation is based on the UNO2 scheme with GSE alleviation based on the cell averaging scheme of Tolman (2002). Currents were applied to the model using the 7km NEMO model outputs (O'Dea et al., 2017). In this regional application ST4 BETAMAX was tuned to 1.45.

2.2.3 Atlantic Margin 3-1.5km model

This configuration (hereon termed UKSCO7) is designed for forecasting shelf seas around the UK, with the intent of providing improved predictions for inshore waters (designated for the UK as within a 12 mile limit of the coastline). The model uses a rotated SMC grid (based on a north pole at 177.50°E 37.50°N) in order to achieve an evenly spaced mesh around UK. Two levels of refinement are applied, at approximately 3 and 1.5km. For this configuration the refinement criterion is based on both proximity to the coast and water depth; 1.5km cells are used for all locations where averaged depths are less than 40m. The grid covers a region from approximately 45°N, 20°W to 63°N, 12°E and is derived from a 1.5km NEMO configuration (Graham et al., 2017); the wave model is forced using surface currents from this model which have been interpolated to the 3km cell scale for compatibility with the base resolution SMC grid cells. Propagation uses the same method as described for the global wave model. ST4 BETAMAX is set to 1.45, as for the AMM7CO6 model.

2.3 Comparison of grids and outputs

Figure 1 illustrates the variations in the grid layouts for the coastal region, in this case for the southwest approaches to England and Wales. Key points of interest are the number of grid cells packed into embayments for the different models and also where the alignment of the grids lead to 'steps' in the rectangular cells adjacent to the coast. Where these steps occur, the flux of shore parallel wave energy may be incorrectly represented by the finite difference propagation scheme, since this operates in the x-y grid directions only.

The AMM7CO6 grid (Figure 1, top right) has, in principle, the poorest representation of sheltered coastal embayments due to a lower density of grid cells; although exposed stretches of coast are reasonably well defined. The S36125 grid (Figure 1, top left) increases the density of cells in the larger embayments, but contains stretches of coast where the grid includes significant steps; for example along the north coast of Cornwall (running southwest to northeast along the southern peninsula shown in the figures). The density of points in sheltered and shallow water embayments is significantly higher in the UKSCO7 model (Figure 1, bottom right). In particular, embayments along the approaches and upper reaches of the Bristol Channel are much more highly populated with model points.

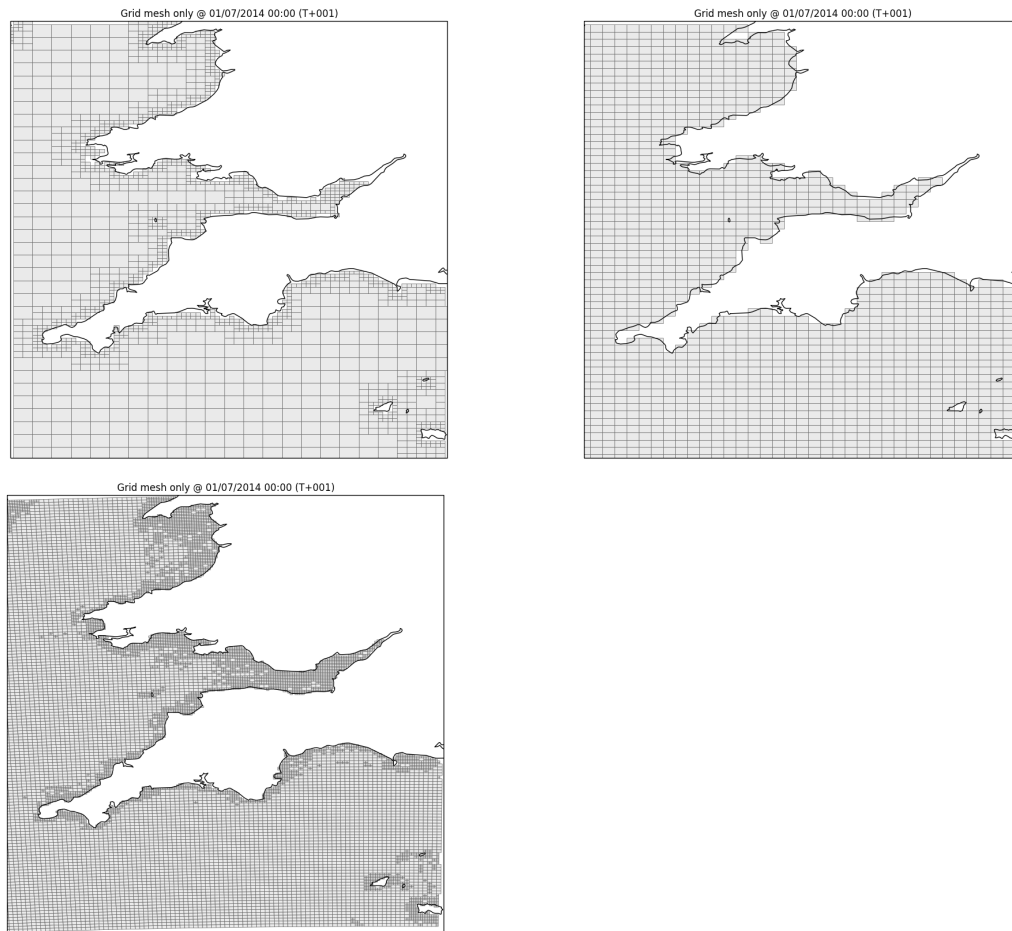


Figure 1. Model grid layouts for approaches to the Bristol Channel. Top left, S36125; top right, AMM7CO6; bottom left, UKSCO7.

Figure 2 shows a zoomed out snapshot of model significant wave height (H_s) fields, in order to illustrate the effect of adding a surface current field. The examples provided are for a slightly wider area of the southwest approaches comprising Atlantic Ocean deep waters, the continental shelf break and shallower waters on the shelf. Compared to the S36125 field which uses no current forcing (Figure 2, top left), AMM7CO6 incorporates some extra detail (Figure 2, top right), whilst the UKSCO7 fields (Figure 2, bottom left) obtain significantly more structure. In both cases this extra structure can be attributed to the current field since all models used the same 17km wind forcing and water depths off the shelf are large (order 1000m). An interesting feature in UKSCO7 field is a set of striations in the vicinity of the continental shelf break in the southwest approaches to the UK. This may be a response to the surface current field generated by internal wave formation over the shelf break. (Mattias Green et al., 2008).

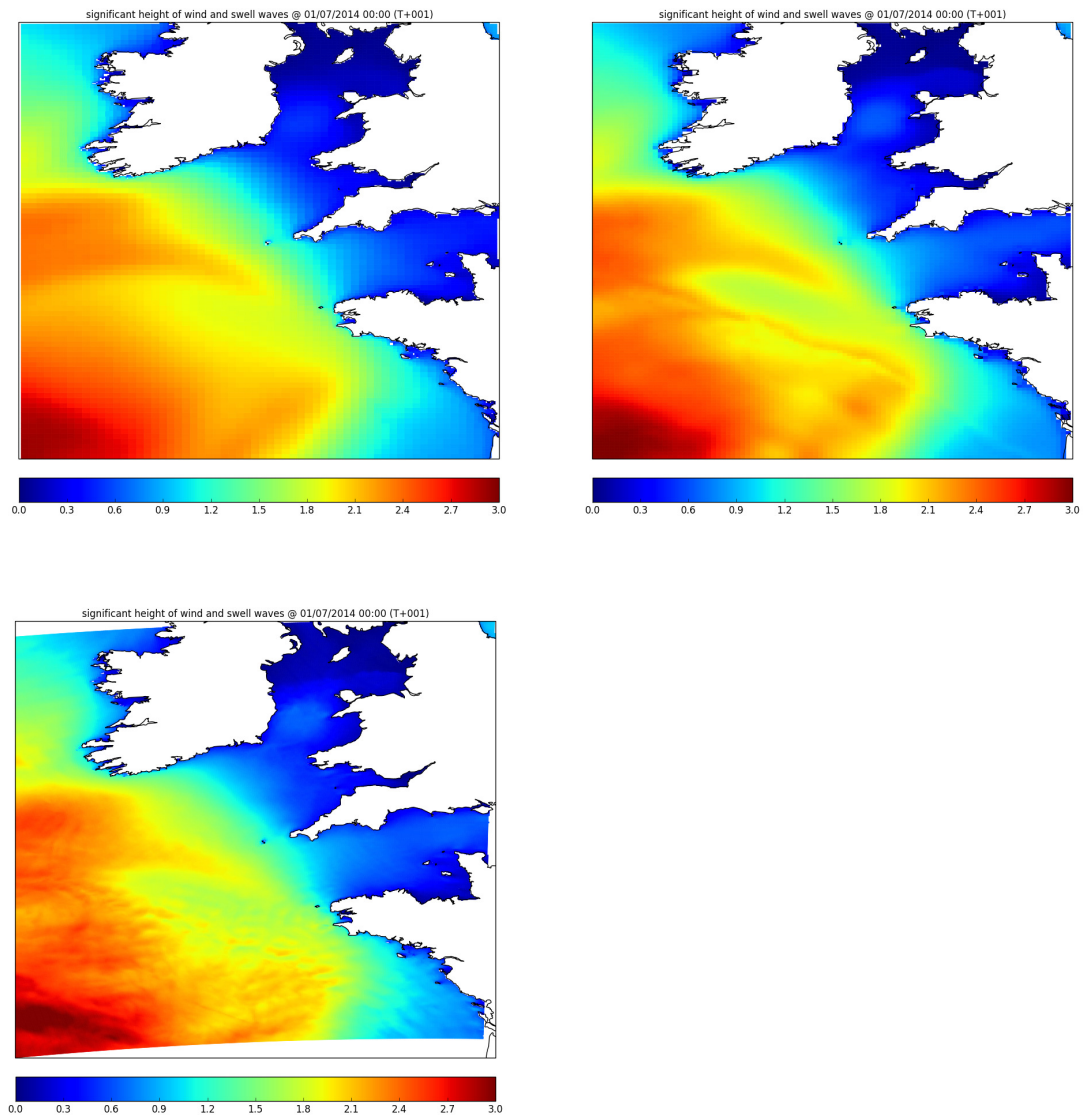


Figure 2. Significant wave height fields for UK southwest approaches. Top left, S36125; top right, AMM7CO6; bottom left, UKSCO7.

3. Trials and observations

3.1 Trials period

The intercomparison covers a summer-early winter period from July 2014 until December 2014. This period was chosen based on availability of both a homogeneous atmospheric analysis (i.e. where no operational model upgrades were applied) and hindcast current data from the 7km and 1.5km ocean models.

3.2 Observation datasets

Validation of the models against observations is focused on in-situ data. Two key sources of data were identified. Data (mostly) covering observations in open waters 10s of kilometres from the coast (from hereon termed offshore data) were sourced from a quality controlled dataset provided to the Met Office under the JCOMM wave forecast verification exchange scheme (WFVS) run by ECMWF (Bidlot et al., 2007). The observations (geographic distribution in Figure 3, lower panel) comprise a mixture of downward pointing lasers/radars, heave sensors and waverider buoys, with match-ups available at 6-hourly intervals. The quality control procedure for these data is described in Bidlot and Holt (2006).

Observations for the coastal zone (geographic distribution in Figure 3, top panel) were sourced from a collection termed WAVENET within the Met Office near real-time observation archives. Observations in this collection comprise, almost exclusively, waverider buoys and are sourced from a number of coastal observatory programs, in particular the Channel Coast Observatory (<http://www.channelcoast.org/>) and the Cefas Wavenet (<https://www.cefas.co.uk/cefas-data-hub/wavenet/>) network of buoys. These data were matched up at an hourly frequency.

For both observation collections, the model match ups were made using a nearest neighbour approach (in both space and time). The model resolutions ensure that all collocations fall within 6km and 20 minutes. Quality control for the verification rejected any match ups where the model-observation difference was greater than 5 times the model background standard deviation.

The relatively high match up frequency for the coastal buoy data is justified based on the likelihood that strong semi-diurnal tidal currents can affect the wave field at coastal locations (e.g. Palmer and Saulter, 2016). In contrast, the wave field further offshore is likely to remain correlated over longer periods, so the lower sample rate for the WFVS data should represent an independent sample. Where overlaps exist in the data collections, verification metrics took similar values. Therefore the choice to compare coastal and offshore verification based on different observation sample rates seems reasonable.

3.3 Metrics

For simplicity, this paper focuses on two key metrics; bias, which indicates systematic errors in model minus observation match-ups, and standard deviation of model-observation errors, which is used as an indication of the model's ability to replicate site based temporal variability in the observed waves. These two metrics represent the simplest breakdown of the root mean squared error statistic.

As one of the focuses of this study is the relative difference in model performance in the offshore and coastal zones, these are presented in normalised form so that a more direct comparison of skill can be made between low energy coastal sites and higher energy offshore locations. In this case, the bias is normalised by the mean observed condition:

$$Bias = \frac{E|X_{model} - X_{obs}|}{E|X_{obs}|}$$

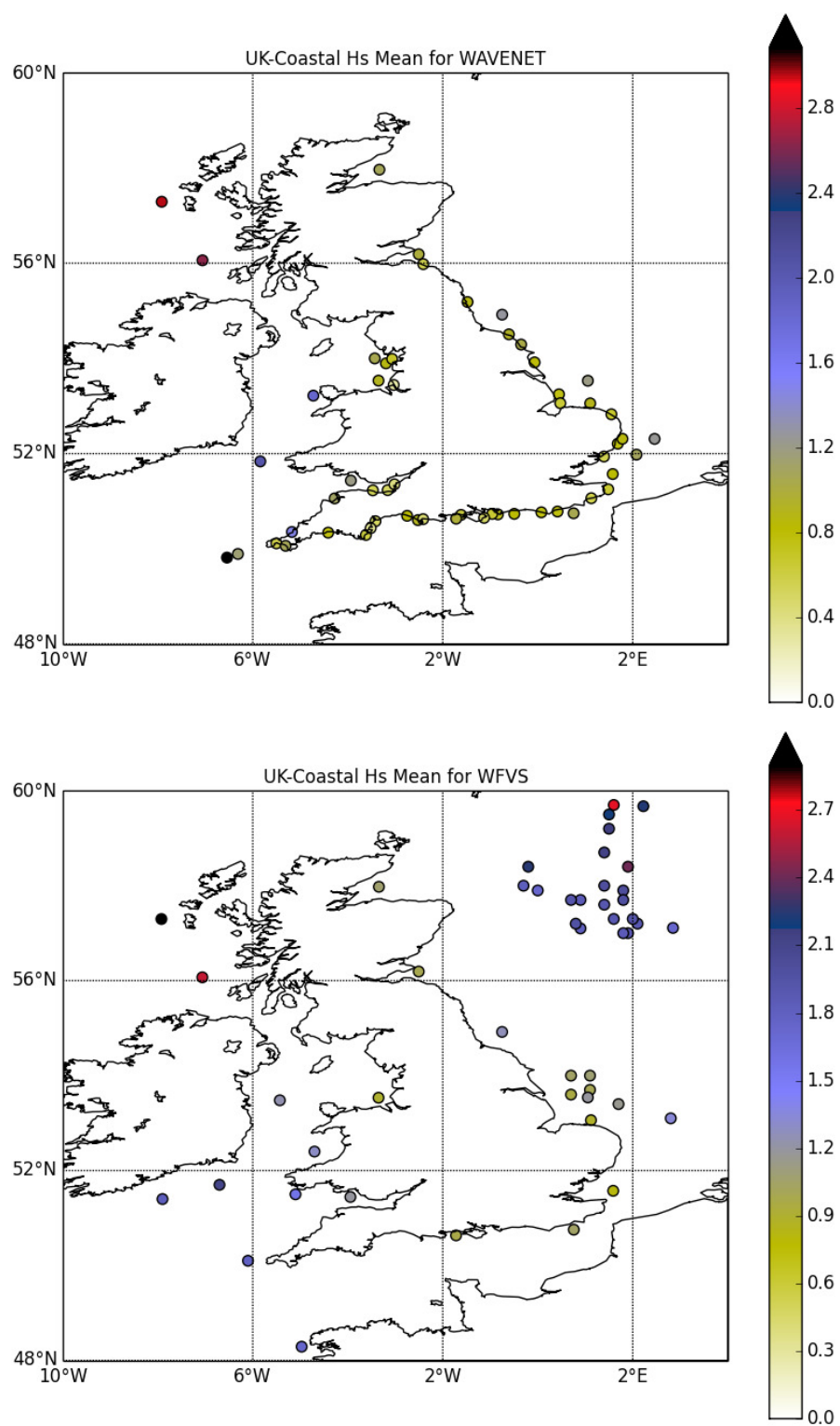


Figure 3. Mean significant wave height (m) from observations for (top panel) WAVENET collection, (lower panel) WFVS collection.

The error standard deviation is normalised by the observed standard deviation, and is termed 'scatter index' (SI) here:

$$SI = \sqrt{\frac{\text{Var}[X_{model} - X_{obs}]}{\text{Var}[X_{obs}]}}$$

It should be noted that scatter index seems, at time of writing, to have no fully agreed definition in the literature (e.g. different forms of normalisation are applied by Bidlot et al., 2002; and Ardhuin et al., 2010). The definition applied here allows SI to be used as a 'skill score', for which a value of 1.0 would be achieved when using the observed mean condition (climatology) as a predictor of time varying behaviour.

4. Intercomparison Results

4.1 Significant wave height

Tables 2 and 3 present statistics summarizing model performance for significant wave height (Hs) prediction in a number of UK waters regions. The regions are defined by clusters of in-situ observation sites and describe some of the different wave climates that can be found in UK waters (e.g. open ocean waters in the UK Northwest Approaches, versus short fetch dominated shallow waters in Liverpool Bay). The best statistic is highlighted in bold for each case.

For the offshore regions (Table 2), little differential can be seen in the statistics achieved by the models and no system consistently outperforms the others. Statistics for the coastal zone (Table 3) are much more variable and the highest resolution configuration, UKSCO7, consistently outperforms the other models. The results in open waters suggest that the key contributions to errors lie more in the quality of forcing wind data and the wave model source terms than in the choice of grid scale or use of currents. In the coastal zone however, the choice of model grid and forcing set up has more impact.

Table 2. By model and region, significant wave height verification statistics for WFVS sites. Observed mean and standard deviation are in metres.

Area	Ob Mean	Ob Std	UKSCO7		AMM7CO6		S36125	
			Norm Bias	SI	Norm Bias	SI	Norm Bias	SI
Celtic-Irish Seas	1.36	0.89	-0.02	0.23	-0.05	0.23	-0.04	0.22
Central North Sea	1.85	1.21	0.00	0.18	0.00	0.18	0.03	0.18
Southern North Sea	1.09	0.65	-0.03	0.24	-0.03	0.25	0.00	0.26
North Sea Approaches	2.46	1.54	0.02	0.21	0.01	0.21	0.02	0.21
UK Northwest Approaches	2.95	1.84	-0.01	0.17	-0.03	0.17	-0.03	0.18
UK Southwest Approaches	2.90	1.56	0.01	0.19	0.00	0.18	-0.01	0.19
English Channel	1.01	0.68	-0.06	0.22	-0.13	0.19	-0.16	0.22
LightVessels	1.78	1.04	0.16	0.22	0.10	0.23	0.14	0.24
Bay of Biscay	1.63	1.06	0.10	0.29	0.01	0.31	0.00	0.30

Table 3. By model and region, significant wave height verification statistics for WAVENET sites. Observed mean and standard deviation are in metres.

Area	Ob Mean	Ob Std	UKSCO7		AMM7CO6		S36125	
			Norm Bias	SI	Norm Bias	SI	Norm Bias	SI
All	0.97	0.89	-0.04	0.22	-0.03	0.33	-0.07	0.29
Southwest Channel	0.75	0.60	-0.01	0.27	0.05	0.48	-0.12	0.28
Southeast Channel	0.75	0.57	-0.06	0.27	-0.08	0.34	-0.09	0.31
Thames Approaches	0.88	0.54	-0.04	0.31	-0.01	0.32	-0.02	0.34
Wash Approaches	0.84	0.51	-0.04	0.31	-0.03	0.34	0.02	0.34
Northeast England	1.07	0.68	-0.08	0.28	-0.04	0.34	-0.12	0.29
Western Isles	2.79	1.91	-0.02	0.16	-0.05	0.17	-0.03	0.17
Liverpool Bay	0.94	0.73	-0.16	0.23	-0.14	0.22	-0.13	0.23
Bristol Channel Approaches	1.39	0.91	-0.02	0.23	-0.08	0.24	-0.16	0.32
Bristol Channel	0.50	0.34	-0.17	0.55	-0.32	0.69	-0.44	0.56

Figures 4 and 5 explore these results in more detail, using a site-by-site approach. In each figure, the map view indicates the relative change in the normalised performance statistic (the absolute value is used for bias) and a large negative value (larger blue symbols) indicates a substantive improvement. The scatterplots below each map compare the statistics at each site directly. In all plots the blue square symbols indicate WFVS data and the green circles are WAVENET data. As an aid to reviewing the data, thresholds have been placed on the scatter plots to indicate levels of 'unacceptable' model performance, i.e. where the statistics suggest that the model either adds little value, or may be misleading in terms of the data it presents. For normalised bias this is set at 0.2 (i.e. model predictions are, on average, different from the observation by more than 20% of the background value) and for SI is set at 0.7 (the model has no little additional skill relative to observed climatology at a value of 1.0).

Bias (Figure 4) shows little or no change between models at all open water sites. At coastal locations the positive impacts of the UKSCO7 are mainly found along the west and south facing coasts, particularly in sheltered embayments facing away from the prevailing wave direction. For UKSCO7 all but three sites have bias within the 'acceptable' range and the biases are much less scattered than for either S36125 or AMM7CO6. This implies a more consistent model performance around the coast for UKSCO7. In contrast, the AMM7CO6 data includes some large outliers where the nearest grid cell poorly represents coastal sheltering effects.

A similar pattern is seen for SI (Figure 5); UKSCO7 is significantly better than the other models for sheltered west and south coast locations and can be deemed skilful at nearly all sites. The improvement between UKSCO7 and S36125 is less marked than in the comparison with AMM7CO6, suggesting that the higher resolution coastal cells in the S36125 model have more of a positive impact on coastal zone significant wave height prediction than the application of currents in the AMM7CO6 model.

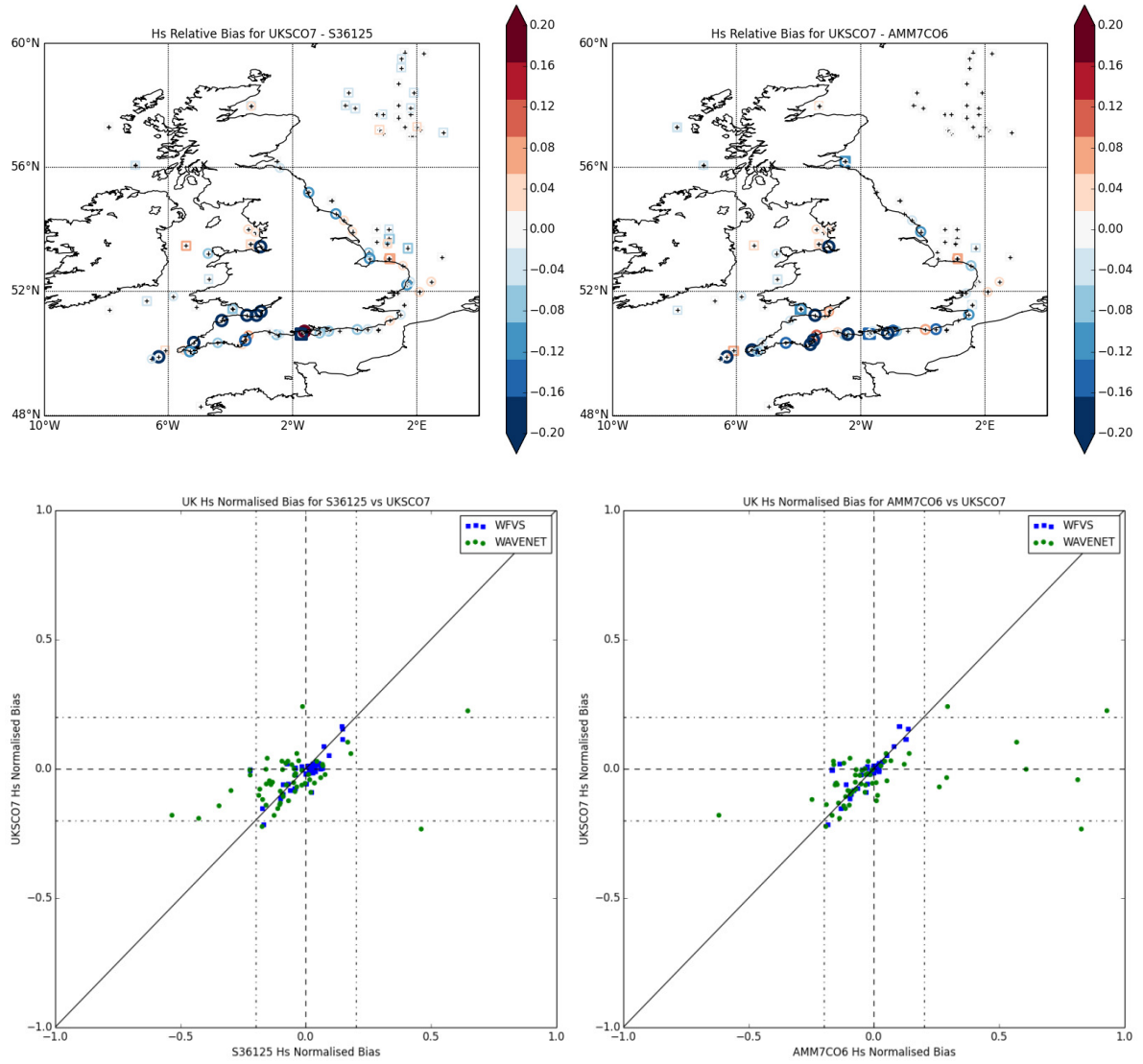


Figure 4. Mapped change in statistic and site by site scatterplot for Hs normalised bias. Left hand side panels: UKSCO7 versus S36125. Right hand side panels: UKSCO7 versus AMM7CO6.

4.2 Wave Period

Tables 4 to 7 present offshore and coastal regional statistics for mean zero-upcrossing (T_{02}) and peak wave period (T_p). For these parameters the AMM7CO6 model is most consistently the best performing. Figure 6 shows that in general there is little to choose between the model bias offshore, but the performance differentials are substantial closer to the coast and the UKSCO7 model improves bias at a number of sheltered sites.

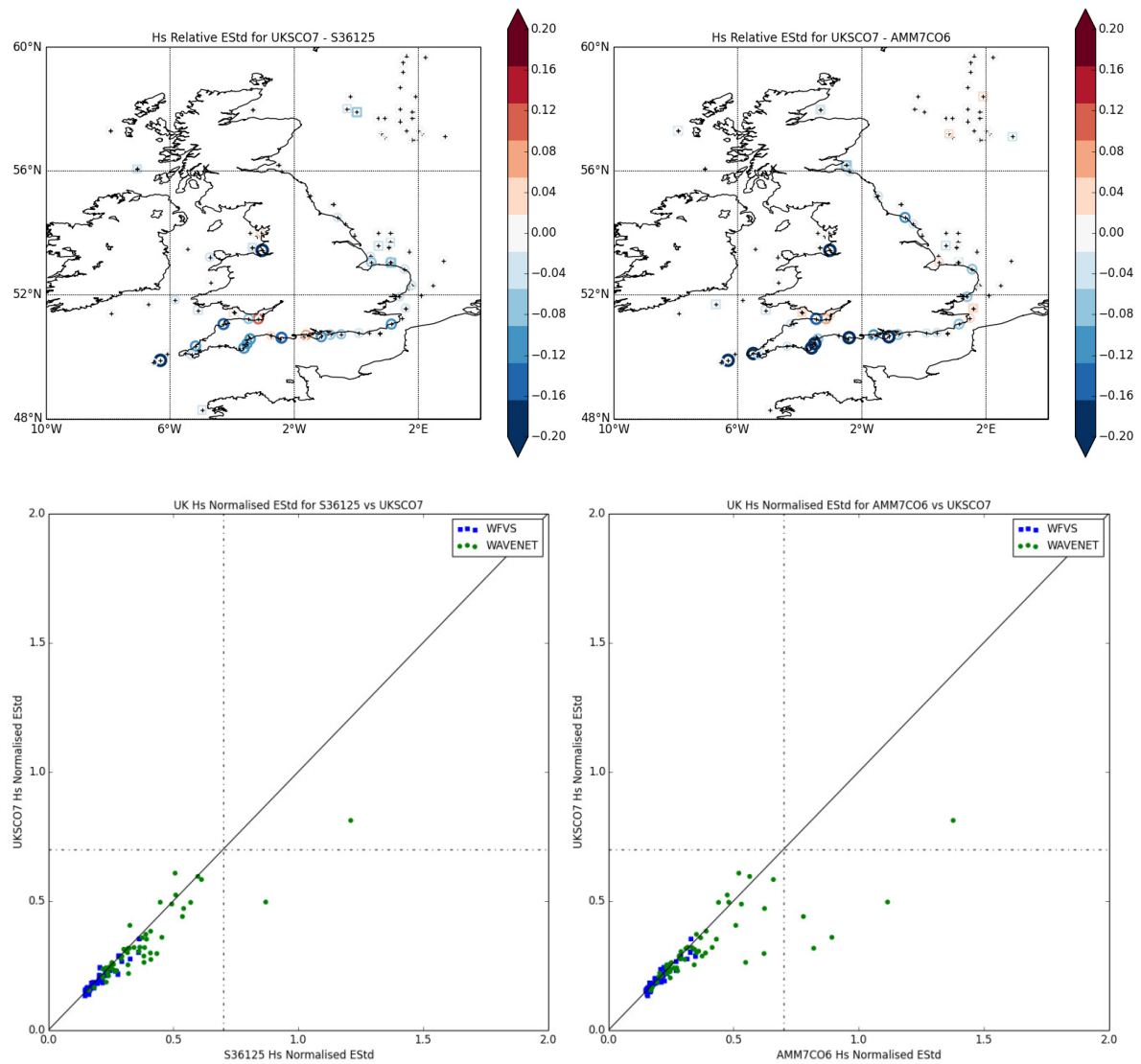


Figure 5. Mapped change in statistic and site by site scatterplot for Hs SI. Left hand side panels: UKSCO7 versus S36125. Right hand side panels: UKSCO7 versus AMM7CO6.

For a number of these locations in the southwest of the UK, SI values are also improved in UKSCO7 (Figure 7). However, SI values are substantially better for S36125 and, particularly, for AMM7CO6 in coastal areas of the Irish Sea and the eastern portion of the English Channel, where currents are relatively strong. UKSCO7 SI values are also slightly worse at the offshore sites. These results are caveated somewhat, due to the generally poor levels of performance for wave period. Many of the coastal sites have an SI of greater than the 0.7 threshold, which is not the case further offshore.

Table 4. By model and region, mean zero-upcrossing period verification statistics for WFVS sites. Observed mean and standard deviation values are in seconds.

Area	Ob Mean	Ob Std	UKSCO7		AMM7CO6		S36125	
			Norm Bias	SI	Norm Bias	SI	Norm Bias	SI
Celtic-Irish Seas	5.00	1.15	-0.06	0.62	-0.10	0.53	-0.09	0.53
Central North Sea	5.34	1.27	-0.07	0.47	-0.09	0.43	-0.08	0.43
Southern North Sea	4.42	0.86	-0.10	0.48	-0.11	0.45	-0.08	0.43
North Sea Approaches	6.36	1.42	-0.09	0.44	-0.10	0.43	-0.10	0.43
UK Northwest Approaches	7.07	1.51	-0.06	0.29	-0.08	0.28	-0.07	0.28
UK Southwest Approaches	6.96	1.54	-0.06	0.30	-0.07	0.28	-0.06	0.29
Bay of Biscay	6.87	1.62	-0.07	0.37	-0.05	0.37	-0.04	0.34

Table5. By model and region, mean zero-upcrossing period verification statistics for WAVENET sites. Observed mean and standard deviation values are in seconds.

Area	Ob Mean	Ob Std	UKSCO7		AMM7CO6		S36125	
			Norm Bias	SI	Norm Bias	SI	Norm Bias	SI
All	4.19	1.29	-0.01	0.75	-0.09	0.71	-0.07	0.74
Southwest Channel	4.25	1.14	0.01	0.94	-0.10	0.93	-0.11	0.98
Southeast Channel	3.65	0.78	0.03	1.30	-0.10	0.99	-0.07	1.14
Thames Approaches	3.75	0.71	-0.10	0.70	-0.12	0.67	-0.09	0.72
Wash Approaches	3.92	0.87	-0.04	0.78	-0.08	0.66	-0.05	0.75
Northeast England	4.62	1.19	-0.04	0.58	-0.11	0.55	-0.09	0.56
Western Isles	6.54	1.66	-0.02	0.32	-0.05	0.31	-0.04	0.30
Liverpool Bay	3.53	0.87	-0.09	0.90	-0.13	0.58	-0.12	0.55
Bristol Channel Approaches	5.33	1.44	0.04	0.72	-0.06	0.71	-0.03	0.76
Bristol Channel	3.50	0.89	0.13	1.82	-0.03	2.16	0.05	2.15

Table 6. By model and region, peak period verification statistics for WFVS sites. Observed mean and standard deviation values are in seconds.

Area	Ob Mean	Ob Std	UKSCO7		AMM7CO6		S36125	
			Norm Bias	SI	Norm Bias	SI	Norm Bias	SI
Celtic-Irish Seas	6.52	2.94	0.10	0.83	0.02	0.65	0.06	0.69
Central North Sea	6.77	2.46	0.06	0.75	0.00	0.70	0.07	0.74
Southern North Sea	6.26	2.28	-0.02	0.80	-0.07	0.67	-0.03	0.80
North Sea Approaches	9.54	2.65	0.04	0.72	-0.02	0.69	0.00	0.68
UK Northwest Approaches	10.36	2.58	0.00	0.48	-0.02	0.47	-0.02	0.48
English Channel	6.65	3.02	0.10	0.68	0.01	0.67	0.05	0.73

Table7. By model and region, peak period verification statistics for WAVENET sites. Observed mean and standard deviation values are in seconds.

Area	Ob Mean	Ob Std	UKSCO7		AMM7CO6		S36125	
			Norm Bias	SI	Norm Bias	SI	Norm Bias	SI
All	6.72	3.24	0.10	0.82	0.01	0.78	0.06	0.81
Southwest Channel	7.51	3.60	0.11	0.84	0.01	0.84	0.03	0.84
Southeast Channel	5.87	2.91	0.22	1.01	0.02	0.86	0.13	0.97
Thames Approaches	5.31	1.62	0.00	0.82	-0.03	0.77	0.04	0.99
Wash Approaches	6.03	2.46	0.06	0.86	0.00	0.72	0.06	0.84
Northeast England	7.48	3.13	0.01	0.67	-0.08	0.72	-0.03	0.66
Western Isles	10.67	2.93	-0.01	0.46	-0.03	0.44	-0.03	0.45
Liverpool Bay	4.68	1.71	0.12	1.68	0.00	1.07	0.04	1.21
Bristol Channel Approaches	9.26	3.11	0.06	0.65	0.00	0.63	0.02	0.65
Bristol Channel	5.39	2.64	0.40	1.20	0.27	1.55	0.38	1.27

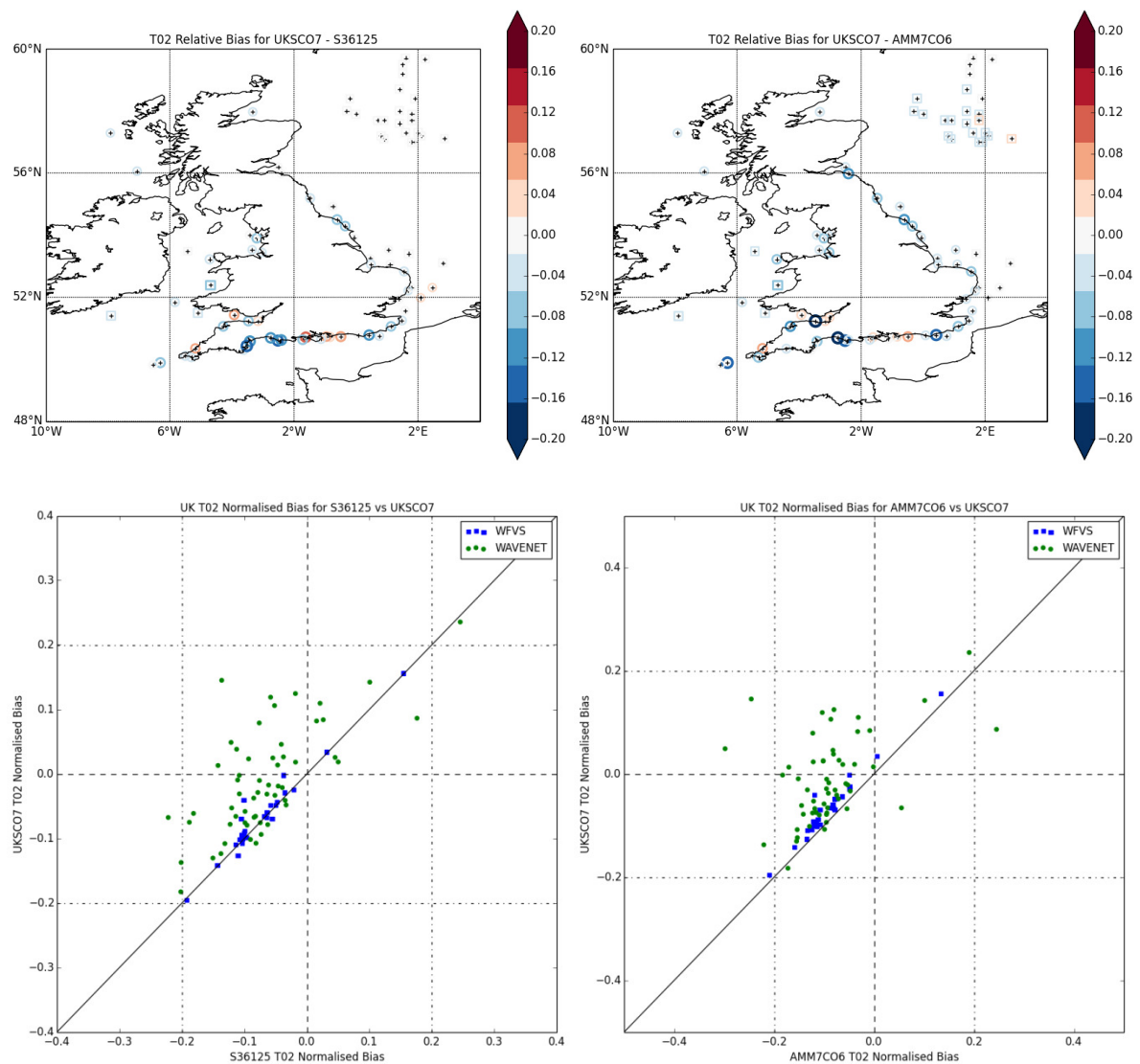


Figure 6. Mapped change in statistic and site by site scatterplot for T02 normalised bias. Left hand side panels: UKSCO7 versus S36125. Right hand side panels: UKSCO7 versus AMM7CO6.

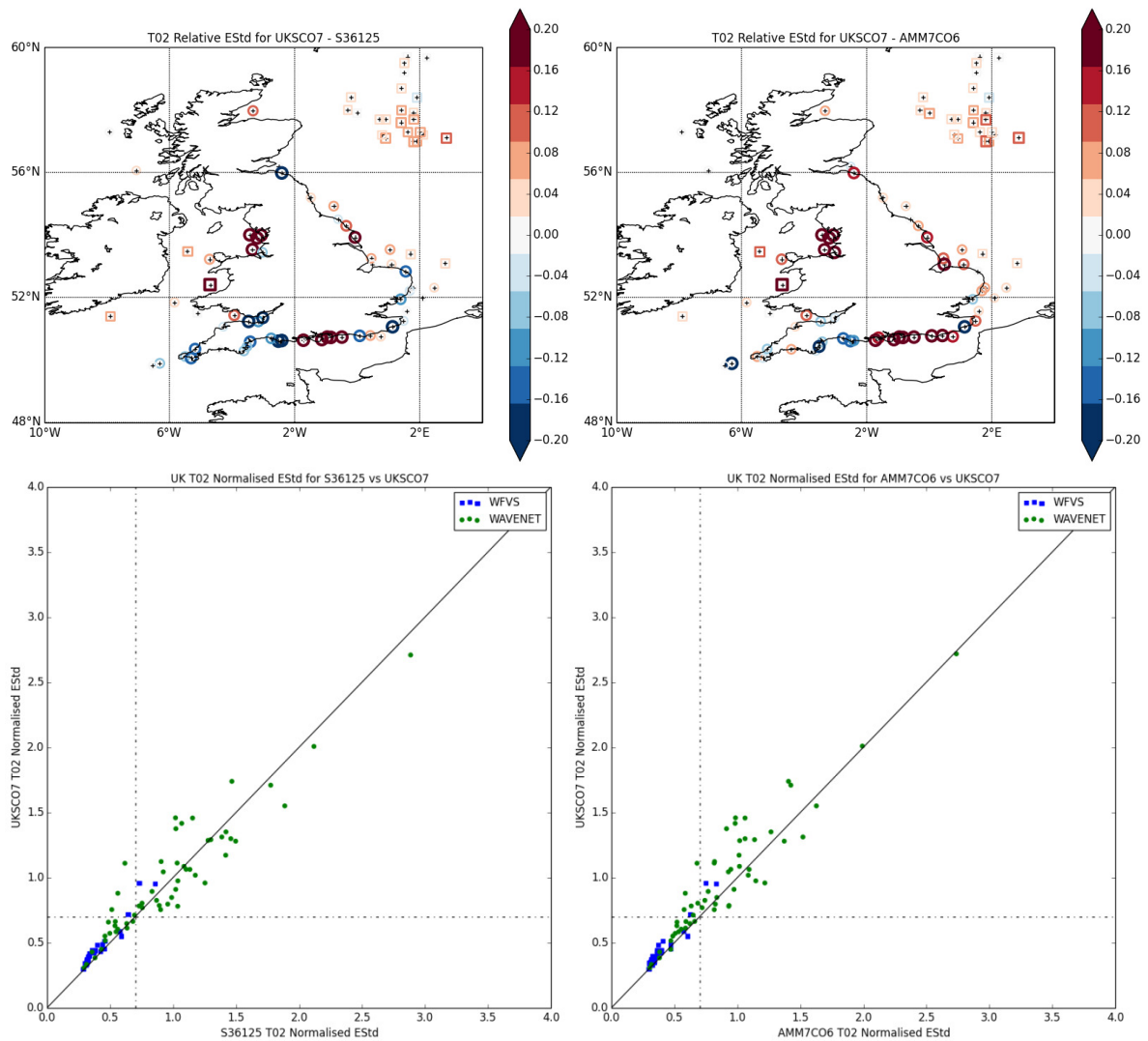


Figure 7. Mapped change in statistic and site by site scatterplot for T02 SI. Left hand side panels: UKSCO7 versus S36125. Right hand side panels: UKSCO7 versus AMM7CO6.

4.3 Offshore versus coastal performance

A clear feature in all of the SI scatterplots is the higher values taken at the coastal buoys. Assuming that the normalisation being applied is equitable across all sites, this implies a comparatively poorer performance from all models for the coastal zone. The differential is particularly marked for wave periods.

The generally poor performance of wave period forecasts and the differentials between the models in the coastal zone are initially illustrated by reviewing time series of data for two coastal locations with particularly high SI values for T02. A time-series for September 2014 at the Cleveleys wave buoy in Liverpool Bay is shown in Figure 8. Although exposed (10km from coast), the location is subject to

long calm periods where H_s is less than 0.4m. At these times measured direction and spread data are variable, as is peak period, whilst measured T_{02} tends to be relatively short. The models generally show more variability in these parameters, with a tendency to overpredict peak wave period and directional spread. The large spread values suggest some bi-modality to the modelled wave spectra which is less apparent in the observations. This may imply that the model systematically overestimates the lower frequency part of the spectrum. These instances will contribute significantly to SI and for the UKSCO7 model occur more frequently for the T_{02} parameter than for the other two models. Conversely, once H_s is at a level of 0.4m or greater the models and observations appear to be very consistent for all parameters; although the comparisons of H_s and T_{02} suggest a small systematic under-prediction of higher frequency wave energy.

Figure 9 shows a time-series for Rustington, which is located in the eastern English Channel and was shown by Palmer and Saulter (2016) to be subject to significant tidal variability and occurrence of bimodal sea-states. These events were associated with refraction of swell from the channel toward the coast. The tidal variability is apparent in observed, UKSCO7 and AMM7CO6 model series. One calm period, with similar characteristics to those identified at Cleveleys, can be seen in the time-series (around 7th September). In other instances directional spread is overestimated by the models, coupled with large overestimates in either T_p or T_{02} . These are indicative of the models predicting bimodal conditions comprising both short period and (refracted) longer period energy, but where the balance between the two components is pushed too far in favour of the longer periods by the models. As for Cleveleys, the impact for T_{02} is largest for the UKSCO7 model. Again, the models and observations are more consistent during more energetic periods (H_s greater than approximately 0.4).

The relationship between wave climate and model performance is explored further in Figure 10, which compares SI for H_s and T_{02} against the observed H_s standard deviation for all three models. The predominance of WFVS data to the right of the x-axis in these plots confirms that the offshore data are generally subject to a higher level of signal (Figure 3 has already shown that the mean H_s is generally higher at the offshore sites). In all cases the SI data decrease with increasing H_s variability and asymptote along the y-axis, where the H_s standard deviation is above approximately 1.0m. SI increases rapidly and is highly scattered for H_s standard deviation less than 0.5m, although the data are more compact for H_s SI in the UKSCO7 and S36125 models. T_{02} shows a similar pattern, but with more scatter and higher values of SI, indicating little or no skill when H_s standard deviation falls below 0.8m. The implication from these results is that increased resolution in the models enables bulk energy to be much better represented in low energy, more sheltered, locations, but has far less impact in terms of the distribution of energy through the wave spectrum. Furthermore, there appears to be a level of energy below which the modelled wave spectrum may be extremely unreliable for predictions.

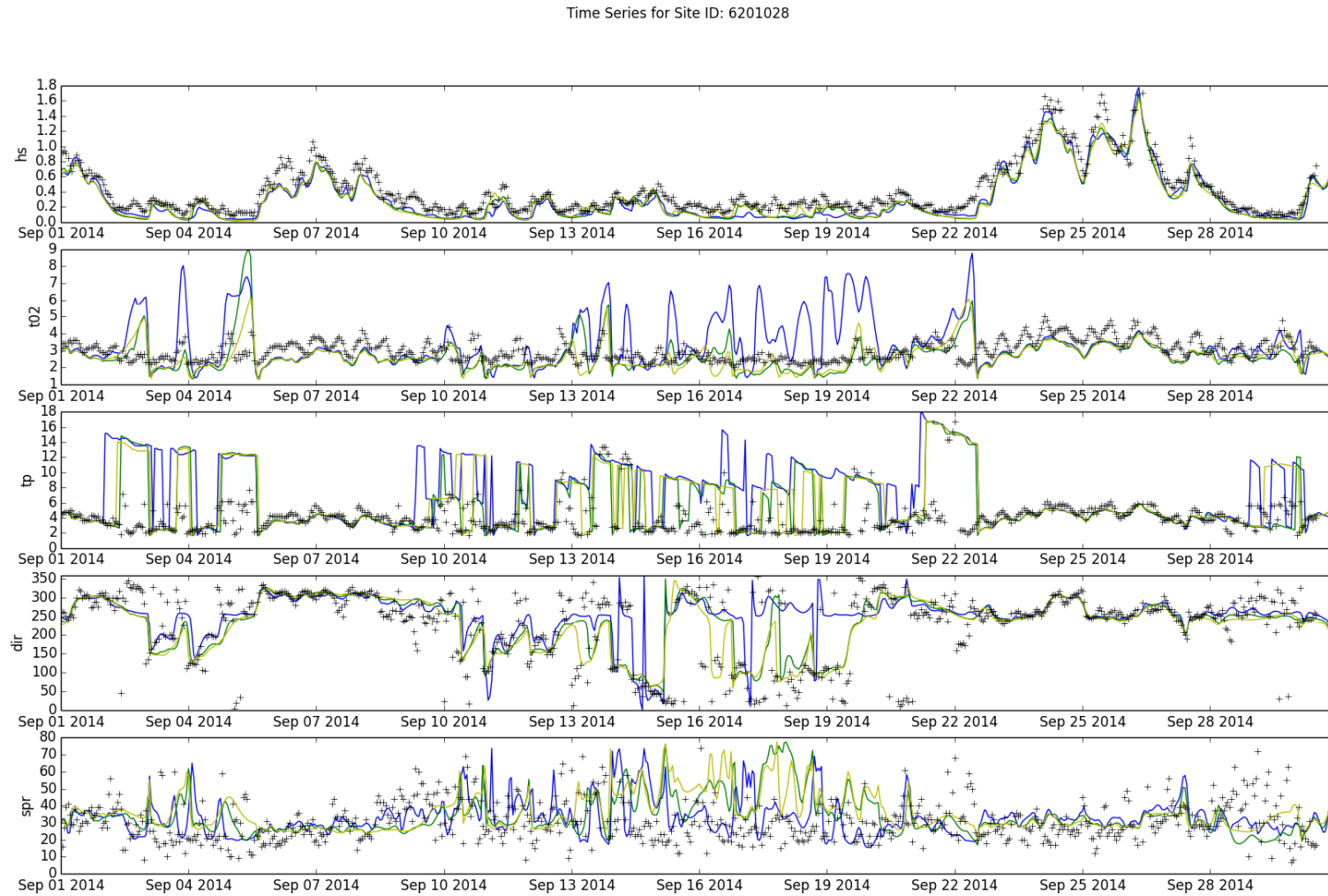


Figure 8. Time series of observations (black crosses), UKSCO7 (blue), AMM7CO6 (green) and S36125 (yellow) model wave parameters for Cleveleys wave buoy.

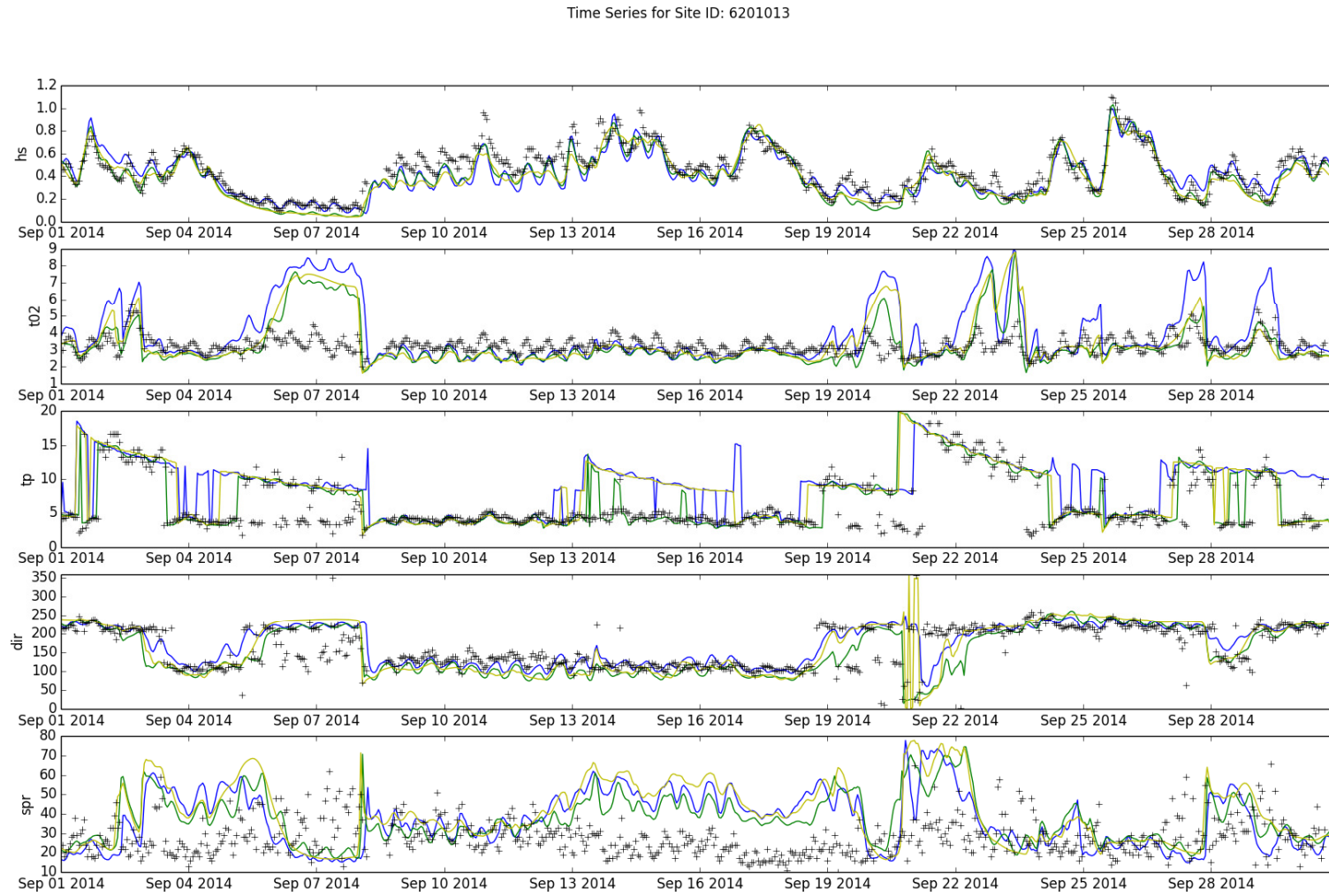


Figure 9. Time series of observations (black crosses), UKSCO7 (blue), AMM7CO6 (green) and S36125 (yellow) model wave parameters for Rustington wave buoy.

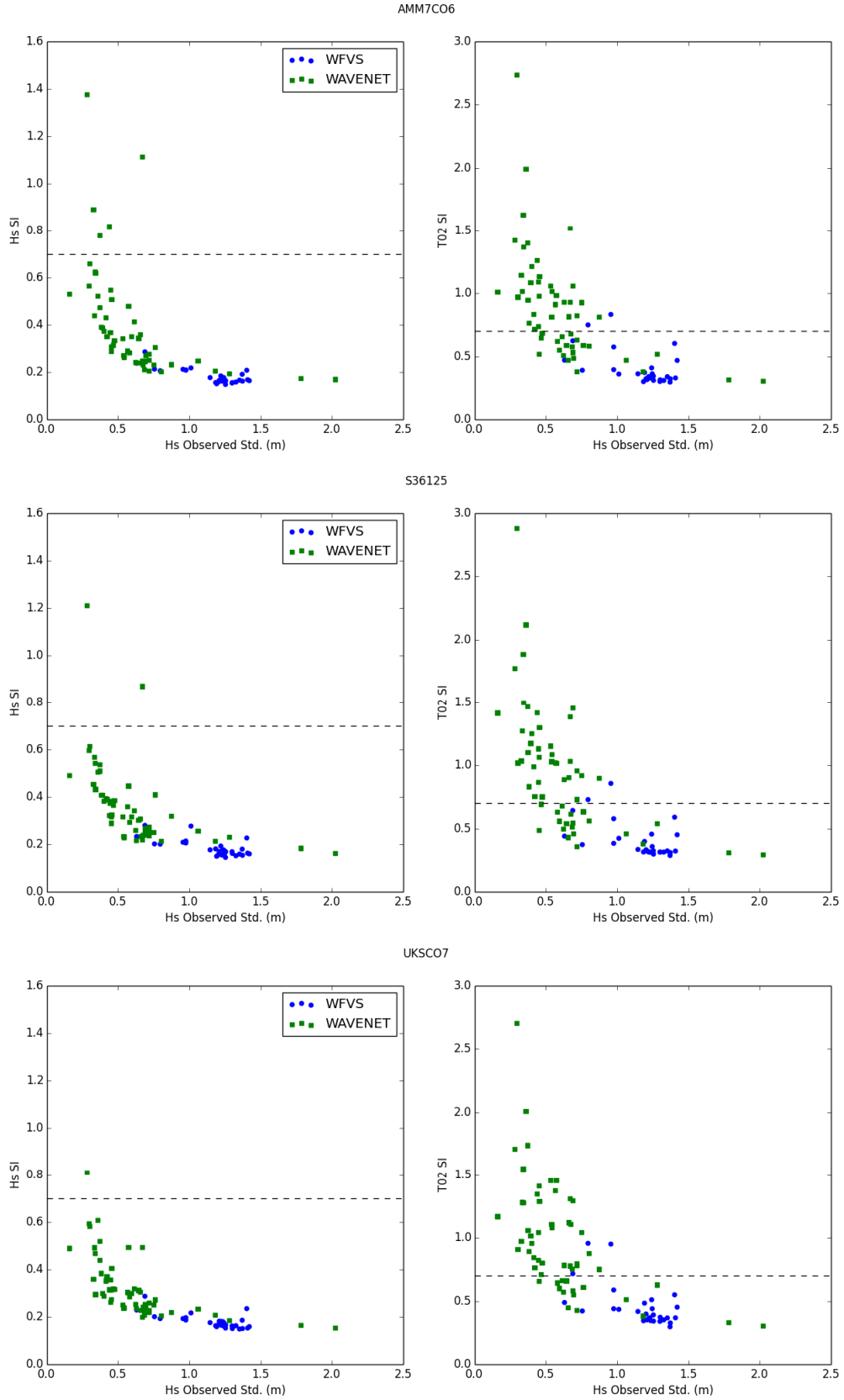


Figure 10. Comparisons of (left) Hs and (right) T02 SI against observed Hs standard deviation for, (top panel) AMM7CO6, (middle panel) S36125 and (lower panel) UKSC07 models.

5. Discussion

In this study measures of model performance against observations have concentrated specifically on systematic bias and standard deviations of model-observation errors. These are simple metrics, which have drawbacks, such as the very high impact of large differentials in wave period in low energy conditions. However the results are relevant because they directly quantify the differentials that a user of these forecasts would experience. Where there are large biases the observed conditions are consistently different from those predicted by the model, whilst large error standard deviations imply that the model is either consistently wrong by a moderate amount, or occasionally wrong by a very large quantity. In whichever case, where poor performance is indicated by these metrics, it means that the forecasts should be used with caution. The use of a normalised form of the metrics based on the observed climate favours sites with a higher energy and more varied climatology (more signal) and models with a low bias and smoother evolution (Mentaschi et al., 2013). Nonetheless, it is believed that the conclusions drawn here regarding differentials between both offshore and nearshore model performance, and between the models themselves, are correct in essence since; a) performance differences between good and bad sites are well marked; and b) the aim of this study was to evaluate whether the models discussed were of the quality necessary to start to consider their non-intervened use in coastal zone applications, since users will tend to judge forecasts in a similar way to that described by the metrics.

With this in mind, significant wave height is generally found to be well predicted by the models; universally offshore and for a majority of coastal locations for the highest resolution model (the UKSCO7, with 1.5km coastal cells). Those sites that were identified as poorly performing all have a common characteristic of being relatively sheltered and within a highly tidal estuary (sites in Liverpool Bay, Bristol Channel). For less complex coastal environments the relative performance of S36125 and AMM7CO6 demonstrate that improving the model resolution is key to achieving a good level of performance. The use of surface current inputs makes a secondary contribution. Results from the UKSCO7 model suggest that the 1.5km resolution used for coastal cells comes close to an optimal resolution needed for generating verifiable UK-wide wave forecasts of significant wave height with an efficient numerical wave model. Offshore, the models are virtually indistinguishable, in line with the common wisdom that wave forecast errors are dominated by the quality of the forcing winds and assumptions underlying the wave source terms (Ardhuin 2012). Where available offshore, statistics for wind SI were in the region of 0.25 to 0.4, so slightly worse than for significant wave height. Due to a lack of observations, no measures of wind quality were available at coastal sites.

Period generally performs more poorly but, caveated by the effect that large period errors under benign wave conditions might have on these types of metrics, performance in open waters is generally skilful. In these locations, better results were achieved by AMM7CO6 and S36125 and it is tempting to speculate that these differentials may be an effect of the current fields used. As shown in Figure 2, the high resolution current field can add significant structure to the wave field. However, in deeper water where this structure has a significant contribution from internal ocean variability (i.e. eddy structures rather than tides), the predictability of the current field is not well quantified. Potentially such features may have a detrimental impact on the UKSCO7 model's performance for these metrics, which can favour 'smoother' models due to so-called double penalty effects. Figure 11 shows an example of the variability in the T02 field in the North Sea (where there is a large

cluster of offshore observations) and the structural difference between AMM7CO6 and UKSCO7 fields are clear. However, there are other potentially significant sources of error to consider. In particular, the comparisons made so far have cast model periods based on relative (intrinsic) frequency (i.e. neglecting the presence of currents) against observed periods based on absolute frequency, since the measurement platforms are in fixed locations.

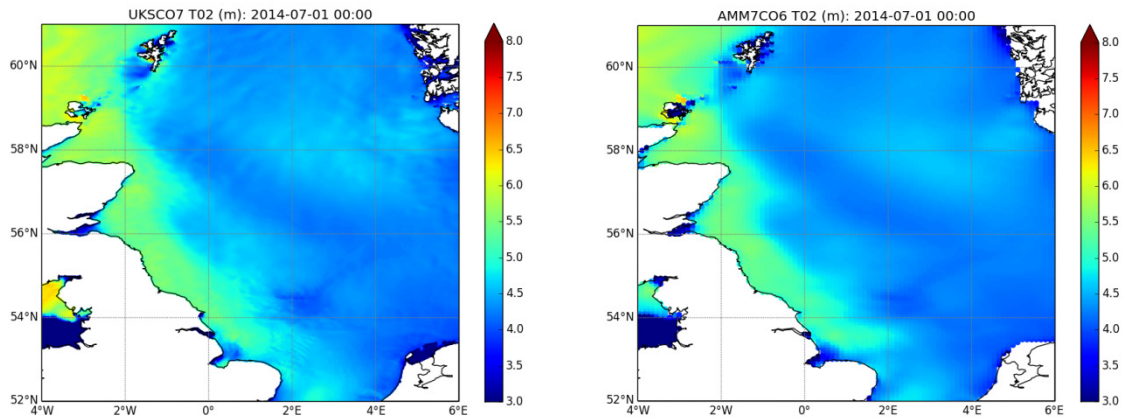


Figure 11. Snapshot of T02 from (left) UKSCO7 and (right) AMM7CO6 models in North Sea

In the coastal zone many of the differences in model performance can be attributed to errors in the detail of underlying wave spectra. A poor representation of the spectrum will affect period and direction parameters much more than the significant wave height. Particular sensitivities are noted in low energy wave conditions and a visual inspection of time-series suggests that the models may over-estimate longer period wave energy and under-predict short period energy. With this in mind, it is possible that the verification for the UKSCO7 highlights these deficiencies more than for the other models; although it is also noted that the main areas where UKSCO7 performs poorly are associated with strong or highly structured current regimes. Further work is required to explore this aspect of performance more closely.

In terms of ‘impact forecasting’, some of the issues highlighted in the coastal zone may be mitigated, since the models seem to generally represent the observed wave parameters better as wave energy increases. A revised analysis for T02 using only observations where H_s was greater than 0.5m led to 15 additional coastal sites giving an acceptably skilful prediction. Nevertheless, significant improvements in coastal zone performance should be targeted, and are available via better process representation in the models. For example, the wind fields used in this study are based on an orography smoothed to the 17km scale. This will fail to capture the full detail of surface roughness associated with the transition zone between sea and land, particularly where coastlines have a high relief. Whilst it is expected that the 1.5km ocean model will begin to replicate some of the structure in strong headland currents, this is unlikely to be achieved fully and may impact tidal variability seen in the coastal wave field. This is illustrated in Figure 12, which shows a time-series for the Bideford

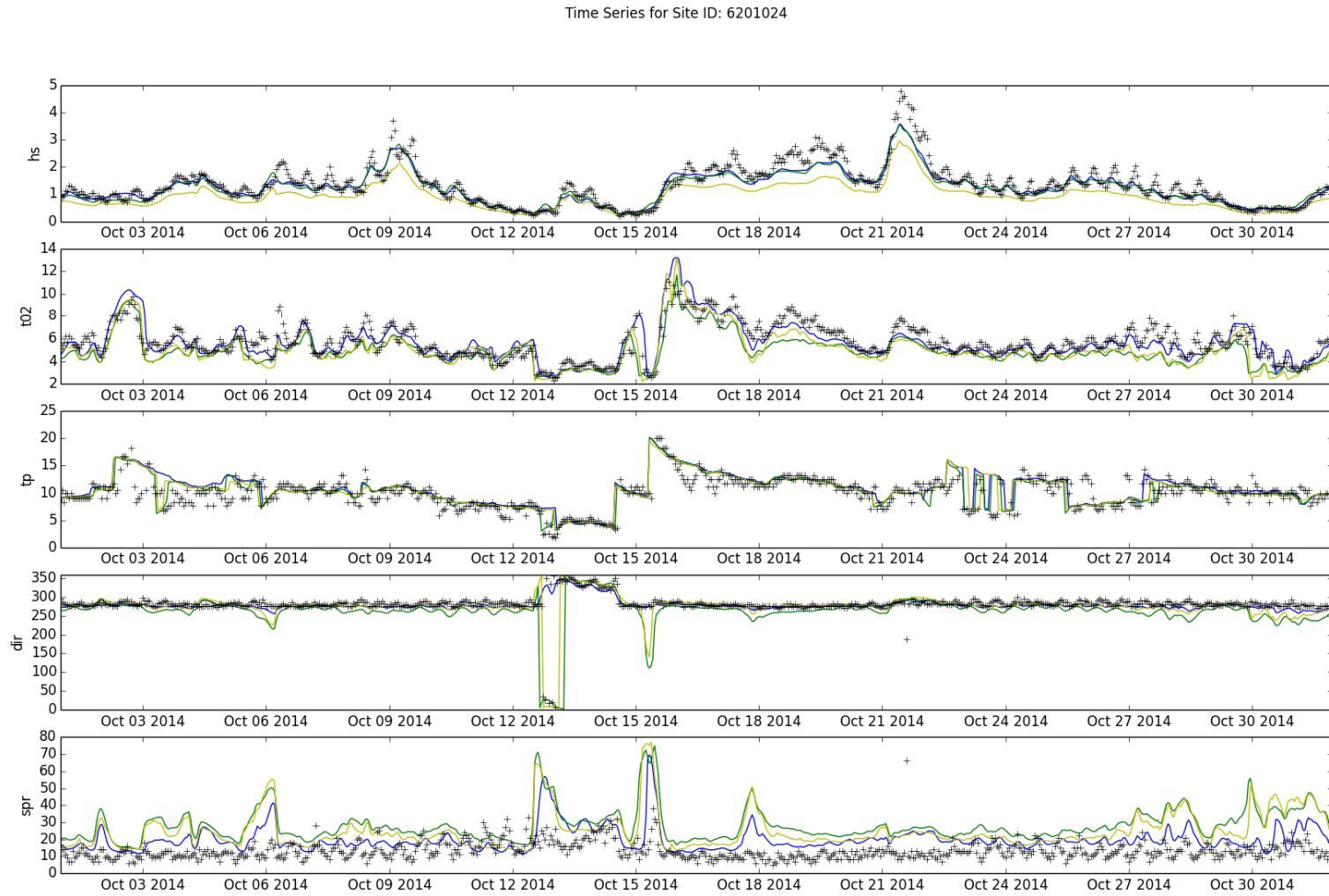


Figure 12. Time series of observations (black crosses), UKSCO7 (blue), AMM7CO6 (green) and S36125 (yellow) model wave parameters for Bideford Bay wave buoy.

Bay wave buoy. This site is embayed and downstream from a relatively strong tidal race in the vicinity of Hartland Point. Variability at tidal frequencies is under-represented during swell dominated conditions, for example the period from October 23rd to October 29th.

Figure 12 also illustrates a grid scale sensitivity that was noted during the study. In this case, the S36125 model systematically under-predicts wave heights, despite resolving the bay better than the AMM7CO6 model. This is attributed to the nearest neighbour selection for the S36125 grid picking a cell that is located on a step in the coastal grid; in this case reducing the flux of energy from directions with both significant south and north components. The nearest cell for AMM7CO6 is better surrounded by grid points, although sited further out into the bay. UKSCO7 also performs better, in this instance for the more correct reason that the nearest grid cell is placed one layer of cells away from the coast and is surrounded by cells on all fetches. Not having to use 'exposed' grid cells is a very simple criterion to guide how well the model is likely to verify in the coastal zone and, therefore, cell selection for forecast applications. Further resolution increases, targeted to achieve such a representation of coastal waters, may require revisions to the parameterisations and numerical schemes used by the wave model (e.g. Huchet et al., 2015).

6. Conclusions

A comparison of three WAVEWATCH III configurations (one global and two regional models), with coastal cell resolutions at 1.5, 3 and 7km scales and varying use of surface current forcing, has been used to illustrate the present capacity for such models to replicate both offshore and coastal wave observations. The skill of all configurations in open waters 10s of kilometres from the coast is very similar, indicating that the principle sources of model error lie with the forcing atmosphere field and wave model source term parameterisations.

In contrast, improving model resolution and applying surface current forcing has a positive impact on coastal zone forecasts of bulk wave energy, as represented by the significant wave height parameter. Of the two model enhancements, improving resolution has the higher impact, particularly where a high cell density significantly changes the representation of sheltered embayments.

Other parameters that have a higher sensitivity to the distribution of wave energy through the spectrum, such as period, show little or no improvement between configurations based on the simple metrics used in this study. Moreover, the metrics suggest that the models have little or no skill in the coastal zone. More detailed review of time-series suggest that the majority of model-observation mismatches occur during low energy, multi-modal wave conditions, which are more common close to the coast than offshore. For more energetic scenarios, the models are capable of replicating observations reasonably well. Nevertheless, numerous aspects of the wave model configuration, forcing and parameterisations can be improved in order to achieve the aim of generically forecasting waves in waters only a few kilometres from the coast with good accuracy.

7. References

- Ardhuin, F., E. Rogers, A.V. Babanin, J.-F. Filipot, R. Magne, A. Roland, A. Van der Westhuysen, P. Queffelec, J.-M. Lefevre, L. Aouf and F. Collard, 2010: Semi-empirical dissipation source functions for wind-wave models. Part I: definition, calibration and validation. *J. Phys. Oceanogr.*, 40 (9), 1917–1941.
- Ardhuin, F., S. T. Gille, D. Menemenlis, C. B. Rocha, N. Rascle, B. Chapron, J. Gula, and J. Molemaker, 2017: Small-scale open ocean currents have large effects on wind wave heights, *J. Geophys. Res. Oceans*, 122, doi:10.1002/2016JC012413
- Ardhuin, F., 2012. Dissipation parameterizations in spectral wave models and general suggestions for improving on today's wave models. *Proc. ECMWF Workshop on Ocean Waves*, ECMWF, 25-27 June, 2012. <https://www.ecmwf.int/sites/default/files/elibrary/2012/7799-dissipation-parameterizations-spectral-wave-models-and-general-suggestions-improving-todays.pdf>
- Battjes, J. A. and J. P. F. M. Janssen, 1978: Energy loss and set-up due to breaking of random waves. In *Proc. 16th Int. Conf. Coastal Eng.*, pp.569–587. ASCE.
- Bidlot, J.-R., D.J. Holmes, P.A. Wittmann, R. Lalbeharry and H.S. Chen, 2002: Intercomparison of the performance of operational ocean wave forecasting systems with buoy data. *Wea. Forecasting*, 17, 287–310.
- Bidlot, J.R. and M.W. Holt, 2006: Verification of Operational Global and Regional Wave Forecasting Systems against Measurements from Moored buoys, JCOMM Technical Report No. 30. http://www.jcomm.info/components/com_oa/oa.php?task=download&id=11736&version=1.0&lang=1&format=1
- Bidlot, J.-R., J.-G. Li, P. Wittmann, M. Faucher, H. Chen, J.-M. Lefevre, T. Bruns, D. Greenslade, F. Ardhuin, N. Kohno, S. Park and M. Gomez, 2007: Inter-Comparison of Operational Wave Forecasting Systems. In *Proc. 10th International Workshop on Wave Hindcasting and Forecasting and Coastal Hazard Symposium*, North Shore, Oahu, Hawaii, November 11-16, 2007.
- Cavaleri, L., and M. Sclavo, 1998. Characteristics of the quadrant and octant advection schemes in wave models. *Coastal Eng.* 34, 221–242. [https://doi.org/10.1016/S0378-3839\(98\)00027-1](https://doi.org/10.1016/S0378-3839(98)00027-1)
- Doorn, N. and R.C. Ris, 1998: Validation of wave propagation on curvilinear grids in SWAN. TU Delft Hydraulic Engineering Reports, <http://resolver.tudelft.nl/uuid:3e5b918f-e84c-476b-925f-b61fe396f113>
- Graham, J. A., E. O'Dea, J. Holt, J. Polton, H.T. Hewitt, R. Furner, K. Guihou, A. Brereton, A. Arnold, S. Wakelin, J.M. Castillo Sanchez and C.G. Mayorga Adame, 2017: AMM15: A new high resolution NEMO configuration for operational simulation of the European North West Shelf, *Geosci. Model Dev. Discuss.*, <https://doi.org/10.5194/gmd-2017-127>, in review.
- Hasselmann, K., T. P. Barnett, E. Bouws, H. Carlson, D. E. Cartwright, K. Enke, J. A. Ewing, H. Gienapp, D. E. Hasselmann, P. Kruseman, A. Meerburg, P. M'uller, D. J. Olbers, K. Richter, W. Sell and H. Walden, 1973: Measurements of wind-wave growth and swell decay during the Joint North Sea

- Wave Project (JONSWAP). Ergänzungsheft zur Deutschen Hydrographischen Zeitschrift, Reihe A(8), 12, 95 pp.
- Hasselmann, S., K. Hasselmann, J.H. Allender, and T.P. Barnett, 1985: Computations and parameterisations of the nonlinear energy transfer in a gravity wave spectrum. Part 2: Parameterisations of the nonlinear energy transfer for application in wave models. *J. Phys. Oceanogr.*, 15, 1378-1391.
- Huchet, M., F. Leckler, J.F. Filipot, A. Roland, F. Ardhuin, M. Dutour Sikiric, H. Michaud, M.T. Delpey and G. Dodet, 2015: High resolution modeling of nearshore wave processes using new implicit scheme of WAVEWATCH III. Proc. 14th International Workshop on Wave Hindcasting and Forecasting and Coastal Hazard Symposium, Key West, Florida, November 8-13, 2015.
http://www.waveworkshop.org/14thWaves/Papers/W2_2015_Huchet_et_al_WAVE_v2.pdf
- Li, J.-G., 2008: Upstream Non-Oscillatory (UNO) advection schemes. *Monthly Weather Review*, 136, 4709-4729.
- Li, J.-G., 2011: Global transport on a spherical multiple-cell grid. *Monthly Weather Review*, 139, 1536-1555.
- Li, J.-G., 2012: Propagation of ocean surface waves on a spherical multiple-cell grid. *Journal of Computational Physics*, 231, 8262-8277.
- Madec, G., 2008: NEMO ocean engine. Note du Pôle de modélisation, Institut Pierre-Simon Laplace (IPSL), France, No 27, ISSN No 1288-1619.
- Mattias Green, J. A., J.H. Simpson, S. Legg, and M. Palmer, 2008. Internal waves, baroclinic energy fluxes and mixing at the European shelf edge. *Continental Shelf Research*, 28 (7), 937-950.
10.1016/j.csr.2008.01.014
- Mentaschi, L., G. Besio, F. Cassola and A. Mazzino, 2013: Problems in RMSE-based wave model validations, *Ocean Modelling*, Dec 2013, Pages 53-58, ISSN 1463-5003.
- O'Dea, E., R. Furner, S. Wakelin, J. Siddorn, J. While, P. Sykes, R. King, J. Holt, and H.T. Hewitt, 2017: The CO5 configuration of the 7 km Atlantic Margin Model: Large scale biases and sensitivity to forcing, physics options and vertical resolution, *Geosci. Model Dev. Discuss.*,
<https://doi.org/10.5194/gmd-2017-15> , in review.
- Palmer, T. and A. Saulter, 2016: Evaluating the effects of ocean current fields on a UK regional wave model. Met Office Forecasting Research Technical Report 612.
http://www.metoffice.gov.uk/media/pdf/j/i/FRTR_612_2016P.pdf
- Roland, A., A. Cucco, C. Ferrarin, T.-W. Hsu, J.-M. Liao, S.-H. Ou, G. Umgiesser, and U. Zanke, 2009: On the development and verification of a 2-D coupled wave-current model on unstructured meshes. *J. Mar. Syst.*, 78, S244–S254.
- Tolman, H. L., 2002: Alleviating the garden sprinkler effect in wind wave models. *Ocean Mod.*, 4, 269–289.

Tolman, H.L., 2008: A mosaic approach to wind wave modeling. *Ocean Modelling*, 25, 35-47.

Tolman, H.L., 2014: User manual and system documentation of WAVEWATCH III® version 4.18.

NOAA / NWS / NCEP / MMAB Technical Note 316, 282 pp + Appendices.

<http://polar.ncep.noaa.gov/waves/wavewatch/manual.v4.18.pdf>

The WAVEWATCH III Development Group., 2016: User manual and system documentation of WAVEWATCH III version 5.16. NOAA / NWS / NCEP / MMAB Technical Note 329, 326 pp. +

Appendices. <http://polar.ncep.noaa.gov/waves/wavewatch/manual.v5.16.pdf>